

Structure evolution of hydroxyapophyllite-(K) under high pressure

Yurii V. Seryotkin (✉ yuvs@igm.nsc.ru)



V.S. Sobolev Institute of Geology and Mineralogy

Research Article

Keywords: Hydroxyapophyllite-(K), fluorapophyllite-(K), apophyllite group, X-ray diffraction, high pressure, structural evolution

Posted Date: September 21st, 2023

DOI: <https://doi.org/10.21203/rs.3.rs-3353727/v1>

License:   This work is licensed under a Creative Commons Attribution 4.0 International License. [Read Full License](#)

Additional Declarations: No competing interests reported.

Version of Record: A version of this preprint was published at Physics and Chemistry of Minerals on January 28th, 2024. See the published version at <https://doi.org/10.1007/s00269-023-01265-2>.

Abstract

The high-pressure structural evolution of a natural hydroxyapophyllite-(K) $K_{0.96}Ca_{4.01}[Al_{0.01}Si_{7.99}O_{20}]((OH)_{0.95}F_{0.05})\cdot(H_2O)_{8.14}$, $Z = 2$, $a = 8.9699(1)$, $c = 15.8934(3)$ Å, space group $P4/mnc$, from the Hatrurim Basin, Negev Desert, compressed in penetrating (ethanol:water 8:1 mixture) medium up to 5 GPa, was studied by single-crystal X-ray diffraction with a diamond anvil cell. The results clearly demonstrate the absence of pressure-induced hydration in the structure. Within 3 GPa the compression mechanism is similar to that known in fluorapophyllite-(K). The compression in the plane of silicate layer proceeds via the relative rotation of the 4-membered rings. The compression along the c -axis proceeds through the shortening of the interlayer distance, whereas the thickness of silicate layer remains almost unchanged. As a result, the pressure-induced changes in the unit cell metrics are similar to those for fluorapophyllite-(K). At about 3 GPa hydroxyapophyllite-(K) undergoes a phase transition with the symmetry lowering to orthorhombic (space group $Pnmm$). The symmetry of the high-pressure phase allows deformation of the four-membered rings of the silicate layer, which is impossible within tetragonal symmetry. In this case, the structure is compressed much more along the a -axis than along the b -axis. As a result, the orthorhombic phase of hydroxyapophyllite-(K) is more compressible compared to fluorapophyllite-(K).

Introduction

Apophyllite-type compounds with general formula $AB_4(Si_8O_{20})X\cdot(H_2O)_8$ ($A = K, Na, NH_4, Cs$; $B = Ca$ (in apophyllite rootname members), Sr (in mcglassonite rootname member); $X = F, OH$) are the specific group of phyllosilicate minerals. Silicate layers are composed of the four- and eight-membered tetrahedral rings; the inter-layer space is filled with cations coordinated, along with the O-atoms of silicate layers, by the H_2O molecules and anions (F^- , $(OH)^-$). Large cations determine a tetragonal symmetry of the apophyllite group minerals (Colville et al. 1971; Rouse et al. 1978; Agakhanov et al. 2019; Števkó et al. 2020), while the symmetry of the Na variety is orthorhombic (Maysueda et al. 1981). Though the minerals of the apophyllite group belong to layered silicates, in their properties they are in many ways similar to the framework water-bearing aluminosilicates – zeolites (Marriner et al. 1990; Fan et al. 2013). This is due to the peculiarities of their structure, such as the presence of silicate layer capable of deformation via mutual rotation of the tetrahedra forming it, as well as the presence of water-cation assemblages in the inter-layer space.

Zeolites are open systems capable of interaction with the environment. Under the compression in water-containing (penetrating) medium, they may experience additional pressure-induced hydration (PIH) (Lee et al. 2002). The PIH effect manifests variously, from the decrease of the compressibility (Arletti et al. 2010; Seryotkin 2015, 2022) to an abrupt expansion of the structure (Belitsky et al. 1992; Seryotkin et al. 2005; Seoung et al. 2013; Seryotkin et al. 2016). The absence of the additional pressure-induced hydration is also possible (Comodi et al 2003; Gatta and Lee 2007; Seryotkin 2019).

The crystal–fluid interaction has been studied in sufficient detail in the case of zeolites (Gatta et al. 2018), whereas the high-pressure behavior of phyllosilicates, including the apophyllite-type compounds, was studied much less. Nevertheless, the compressibility of two minerals of the apophyllite group,

fluorapophyllite-(K) in pure water (Kim et al. 2015) and hydroxyapophyllite-(K) in nominally penetrating medium (Fan et al. 2013) was studied by powder X-ray diffraction methods. Recently we have investigated the structural evolution of fluorapophyllite-(K) under the compression up to 5 GPa in penetrating (water-containing) and non-penetrating medium (Seryotkin and Ignatov 2023). The mineral composition was constant within the whole pressure range, and the compressibility was found similar in both media; it follows that fluorapophyllite-(K) does not undergo the pressure-induced hydration.

The comparison of the obtained results with the literature data shows that the compressibility of hydroxyapophyllite-(K) in “nominally penetrating medium” (Fan et al. 2013) is appreciably lower than that of fluorapophyllite-(K) (Seryotkin and Ignatov 2023). Such difference in the compressibility is commonly explained by the additional hydration under the compression in penetrating medium. However, taking into account exceptional structural similarity of hydroxyl- and fluorine-bearing compounds, this can hardly be expected. Such uncertainty motivated us to study the behavior of hydroxyapophyllite-(K) under the compression in water-containing medium.

The aim of the present work is to elucidate the peculiarities of the high-pressure structural evolution of hydroxyapophyllite-(K) relative to fluorapophyllite-(K).

Experimental

Hydroxyapophyllite-(K) from the Hatrurim Basin, Negev Desert (Sokol et al. 2014) was provided by Ella Sokol. The chemical analyses were carried out at the Analytical Center for Multi-Elemental and Isotope Research (Sobolev Institute of Geology and Mineralogy (IGM), Novosibirsk, Russia) using Tescan Orsay *TESCAN MIRA 3LMU* microscope equipped with an Oxford Instruments AZtec Energy XMax-50 microanalyzer (Abingdon, UK) at 1.5 nA and 20 kV and counting time of 20 s. The strategy of analysis is described by Lavrent'ev et al. (2015). The water content was measured by thermogravimetric analysis using Mettler TA3000 equipment (temperature range 20–750°C, heating rate 10°C/min). Resulting composition is $K_{0.96} Ca_{4.01} [Al_{0.01} Si_{7.99} O_{20}] ((OH)_{0.95} F_{0.05})_{\Sigma 1.00} \cdot (H_2O)_{8.14}$.

A 0.22×0.19×0.05 mm tabular crystal without visible defects was chosen for the X-ray diffraction study. Diffraction data at ambient conditions (in air) were collected on X-ray Oxford Diffraction Xcalibur Gemini diffractometer (MoK α , ω -scan with a stepsize of 1°, 30 s per frame). Data reduction was processed using *CrysAlis Pro* 1.171.42.49 program package (Rigaku Oxford Diffraction 2022). A semi-empirical absorption correction was applied using the multi-scan technique. The structure was solved with the SHELXS (version 2013/1) and refined with the SHELXL-2018/3 software (Sheldrick 2015). The positions of hydrogen atoms were located in a difference Fourier maps. All non-hydrogen atoms were refined with anisotropic displacement parameters.

The high-pressure experiments were performed in Boehler-Ahsbahs type diamond anvil cell (DAC, Boehler 2006) with the 600 μ m diameter culets. The 200 μ m thick stainless steel was used as the gasket material, indented to 110 μ m and drilled to obtain a sample chamber with diameter of 320 μ m. Pre-characterized crystal was placed inside the sample chamber along with the ruby sphere for pressure calibration (± 0.05

GPa) (Piermarini et al. 1975). An ethanol:water (8:1) mixture was used as a *P*-transmitting medium. Data were collected with 0.5° ω -scan step and 45 s of exposure time per frame, with the strategy of *CrysAlis Pro* for the high-pressure experiments in DAC. In total, data were accumulated at nine points on the pressure rise and at two more points on the reverse. Then the sample was removed from the DAC, and the diffraction data were collected to estimate the reversibility of pressure-induced changes in the structure.

The collected diffraction data were reduced using the *CrysAlis Pro* software. The structures were refined using the SHELXL-2018/3 package; the structural parameters obtained for the previous pressure point were set as the starting model. Above 4 GPa the crystal quality significantly deteriorated; the results of structure refinement at the last pressure point (4.93 GPa) seem not reliable. Therefore the structure data for this pressure point are omitted.

The unit-cell parameters at high pressure are presented in Table 1. Complete experimental details of data acquisition and structure determination are listed in Tables 2 and 3. The results of structural refinement are given as Supplementary materials (Tables S1–S4 and CIF files).

Table 1
Lattice parameters, unit-cell volume, and space group for hydroxyapophyllite-(K).

P, GPa	a, Å	b, Å	c, Å	V, Å³	Space group
0.0001*	8.9699(1)		15.8934(3)	1278.78(4)	<i>P4/mnc</i>
0.25	8.9500(1)		15.853(4)	1269.8(3)	<i>P4/mnc</i>
1.23	8.8779(1)		15.760(4)	1242.2(4)	<i>P4/mnc</i>
1.77	8.8438(1)		15.726(4)	1230.0(4)	<i>P4/mnc</i>
2.24	8.8113(1)		15.696(5)	1218.6(4)	<i>P4/mnc</i>
2.72	8.7863(1)		15.667(5)	1209.4(4)	<i>P4/mnc</i>
3.09	8.7530(3)	8.7676(3)	15.652(7)	1201.2(5)	<i>Pnmm</i>
3.55	8.7294(3)	8.7532(4)	15.595(9)	1191.6(7)	<i>Pnmm</i>
4.64	8.6552(6)	8.7349(8)	15.519(14)	1173.3(11)	<i>Pnmm</i>
4.93	8.6345(8)	8.7306(9)	15.508(18)	1169.1(14)	<i>Pnmm</i>
4.14**	8.6955(5)	8.7451(6)	15.545(12)	1182.1(9)	<i>Pnmm</i>
0.70**	8.9126(2)		15.819(8)	1256.6(7)	<i>P4/mnc</i>
0.0001#	8.9704(1)		15.8939(4)	1278.94(5)	<i>P4/mnc</i>

* in air.

** under decompression.

after decompression, in air.

Table 2

Parameters of data collection and structure refinement for low-pressure phase of hydroxyapophyllite-(K).

Pressure (GPa)	0.0001*	0.25	1.23	1.77	2.24	2.72	0.70**	0.0001#
Space group	<i>P4/mnc</i>	<i>P4/mnc</i>	<i>P4/mnc</i>	<i>P4/mnc</i>	<i>P4/mnc</i>	<i>P4/mnc</i>	<i>P4/mnc</i>	<i>P4/mnc</i>
d (g/cm ³)	2.349	2.366	2.418	2.442	2.465	2.484	2.391	2.349
μ (MoK α) (mm ⁻¹)	1.505	1.515	1.549	1.565	1.579	1.591	1.531	1.505
Scan width (°/frame)	1	0.5	0.5	0.5	0.5	0.5	0.5	1
Exposure (s/frame)	30	45	45	45	45	45	45	60
2 θ range (°)	5.13–63.70	5.23–63.22	5.27–63.60	5.28–63.57	5.30–63.52	5.32–63.51	5.25–63.23	5.13–63.81
Number of I_{hkl} measured	23673	9377	9124	9055	8968	8834	8950	23645
Number of unique F^2_{hkl}	1132	475	421	406	387	370	404	1137
R_{int}	0.0508	0.0493	0.0457	0.0467	0.0468	0.0485	0.1222	0.0825
Reflections with $I > 2\sigma(I)$	985	432	386	371	352	329	317	960
Number of variables	62	62	62	62	62	61	62	62
$R1, wR2$ for obs. reflections [$I > 2\sigma(I)$]	0.0255, 0.0635	0.0274, 0.0631	0.0246, 0.0594	0.0244, 0.0597	0.0228, 0.0565	0.0234, 0.0557	0.0469, 0.1029	0.0373, 0.0916
$R1, wR2$ for all data	0.0321, 0.0671	0.0328, 0.0658	0.0292, 0.0616	0.0296, 0.0625	0.0279, 0.0584	0.0281, 0.0588	0.0657, 0.1133	0.0476, 0.0974
GooF	1.090	1.141	1.111	1.191	1.140	1.093	1.063	1.089
Residual electron density (e/ \AA^3)	0.476, -0.341	0.246, -0.280	0.269, -0.211	0.244, -0.269	0.242, -0.268	0.193, -0.227	0.437, -0.362	

* in air.

** under decompression.

after decompression, in air.

Table 3
Parameters of data collection and structure refinement for high-pressure phase of hydroxyapophyllite-(K).

Pressure (GPa)	3.09	3.55	4.64	4.14*
Space group	<i>Pnnm</i>	<i>Pnnm</i>	<i>Pnnm</i>	<i>Pnnm</i>
d (g/cm ³)	2.501	2.521	2.560	2.541
μ (MoK α) (mm ⁻¹)	1.602	1.615	1.640	1.628
Scan width (°/frame)	0.5	0.5	0.5	0.5
Exposure (s/frame)	45	45	45	45
2 θ range (°)	5.33–63.66	5.34–63.33	5.35–63.32	5.34–64.19
Number of I _{hkl} measured	8812	8532	7901	8974
Number of unique F ² _{hkl}	684	680	673	671
R _{int}	0.0477	0.0523	0.1156	0.1306
Reflections with I > 2 σ (I)	564	554	461	488
Number of variables	115	120	113	104
R1, wR2 for obs. reflections [I > 2 σ (I)]	0.0281, 0.0640	0.0333, 0.0677	0.0610, 0.0955	0.0547, 0.1172
R1, wR2 for all data	0.0395, 0.0694	0.0471, 0.0730	0.1061, 0.1119	0.0854, 0.1306
GooF	1.042	1.083	1.045	1.093
Residual electron density (e/ Å ³)	0.256, -0.284	0.287, -0.308	0.444, -0.462	0.384, -0.476
* under decompression				

Results and Discussion

The crystal structure of hydroxylapophyllite-(K) at ambient conditions is shown in Fig. 1. The silicate layers are composed of four- and eight-membered rings of SiO_4 -tetrahedra. Large K^+ cation has no contacts with the tetrahedral layer and is coordinated by eight H_2O molecules arranged in a flattened tetragonal prism. The Ca^{2+} cations are bounded to four apical O atoms of two neighbor tetrahedral layers (two from each layer); the Ca^{2+} coordination also includes two H_2O molecules and hydroxyl group $(\text{OH})^-$, which form, along with the oxygen atoms, single - cap trigonal prism. The (OH) -group is surrounded by four Ca^{2+} cations arranged in a regular flat square as a coordination polyhedron. The proton vector $\text{O}-\text{H}$ is directed along the four-fold symmetry axis; the shortest distances $\text{H}\cdots\text{O}_3$ are 2.61 Å. At that the distance $\text{O}_\text{H}-\text{O}_3$ of 2.950 Å is comparable to 2.947 Å, the value from the literature data (Rouse et al. 1978). The distance $\text{F}-\text{O}_3$ in fluorapophyllite-(K) structure is 2.924–2.928 Å (Chao 1971; Colville et al. 1971; Seryotkin and Ignatov 2023). Note that the volume of hydroxylapophyllite-(K) is somewhat greater than that of the fluorine-bearing variety, which is consistent with the larger distances in its structure. The hydrogen bonds of the H_2O molecules are differentiated, similarly to the structures of other minerals of apophyllite group. A strong hydrogen bond connects H1 and apical atom O3, and a weaker bond links H2 and the bridge atom O2 of the four-membered ring (see Table S3).

At the initial stage (below 1 GPa) the structure compression is almost isometric (Fig. 2). Upon the pressure rise the compression anisotropy increases; for example, at 2.7 GPa the a and c parameters are reduced by 2.0 and 1.4%, respectively.

At about 3 GPa a presumably 1st order phase transition is observed; the symmetry is lowered down to orthorhombic (space group $Pnmm$) and the compressibility along the c axis increases (Fig. 2). The compressibility along the a axis remains similar to that observed at a lower pressure and increases only slightly above 4 GPa, whereas the compressibility along the b axis decreases appreciably (Fig. 2).

Within the region of tetragonal phase (below 3 GPa) the compression mechanism in hydroxylapophyllite-(K) is the same as that revealed in the fluorine-bearing variety (Seryotkin and Ignatov 2023). Within the (xy) plane the compression proceeds via the rotation of the 4-membered rings in silicate layer relative to each other. The 4-membered rings lie on the 4-fold axis, which significantly limits the possibility of changing their geometry. As a result, the rings remain almost undeformed: the distance O_1-O_1 defining the ring dimension shortens from 6.97 Å at ambient conditions to 6.94 Å at 2.72 GPa. The angle $\text{Si}-\text{O}_2-\text{Si}$ at the bridge O-atom of the ring diminishes by only 0.8° in the range of 0.0001–2.72 GPa (Fig. 3), which also evidences for the absence of the rings deformation. The angle $\text{Si}-\text{O}_1-\text{Si}$, defining the mutual rotation of the rings within the layer, decreases by 3.2° within the same pressure region. This results in the decrease of the 8-membered rings aperture from c 3.46 to 3.11 Å. The compression perpendicular to the layers (along the c axis) proceeds due to the shortening of the interlayer space (Fig. 4). The thickness of silicate layer remains constant, similarly to the structure of fluorapophyllite-(K) (Fig. 4).

Note, however, that upon approaching the transition pressure the angle $\text{Si}-\text{O}_2-\text{Si}$ at the bridge O-atom of the 4-membered ring begins to decrease appreciably more than the corresponding angle in the structure of the fluorine-bearing variety: in the latter the angle $\text{Si}-\text{O}_2-\text{Si}$ decreases by only 1.2° at 4.7 GPa, whereas in

hydroxylapophyllite-(K) it diminishes by 1.7° already at 2.7 GPa (Table S3). We cannot exclude that this could provoke the phase transition. As it was mentioned, in the tetragonal structure (space group $P4/mnc$) the 4-membered rings located at the 4-fold axes are practically incapable of deformation. When the symmetry is lowered to orthorhombic (space group $Pnmm$), leading to the respective splitting of one positional system into two independent systems, new ways of deformation of the silicate layer appear. For example, the loss of the four-fold axis makes possible the angular deformation of the 4-membered rings and the layer shrinkage. The ring deformation manifests in the differentiation of the angles Si1–O2–Si2, Si1–O20–Si2 (Fig. 3) and respective distances O2–O2 and O20–O20 in the 4-membered rings; the layer shrinkage is associated with the differentiation of the distances O3–O3 and O30–O30 (Fig. 4). However, their contribution to the structure compression is minor (about 0.01 Å) compared to the rotation of the 4-membered rings. The angular deformation of the rings manifests mainly in the increase of the difference in the a - and b -parameter of the orthorhombic cell.

The coordination of the inter-layer cations is preserved within the whole pressure range studied. The Ca²⁺ coordination includes four O atoms of silicate layer, two H₂O molecules and the (OH)[–] radical. The Ca–H₂O distance in the structure of hydroxylapophyllite-(K) is almost equal to that in fluorapophyllite-(K) (Seryotkin et al. 2023); the distances Ca–O₃ and Ca–O_H are 0.02 Å longer in the (OH)-form. This tendency is preserved under high pressure. The decrease of the interatomic distances with pressure is close to linear. The variations of the mean distances $\langle \text{Ca}-\phi \rangle$ ($\phi = \text{O}, \text{H}_2\text{O}, (\text{OH})^-, \text{F}^-$ – Agakhanov et al. 2019) with pressure in the hydroxy- and fluorapophyllite-(K) (Seryotkin and Ignatov 2023) are plotted in Fig. 5. Upon the phase transition the dependence for the (OH)-form breaks with a slight increase in the average distance $\langle \text{Ca}-\phi \rangle$. At 4.6 GPa the distances Ca–O and Ca–O_w shorten by 2–3%, whereas the Ca–O_H decreases by less than 1%. The K(H₂O)₈ polyhedra are compressed much more: within the same pressure range the K–O_w distances decrease linearly by more than 6% (Fig. 6). Unlike the distances in the Ca-polyhedra, initially the bond K–H₂O in hydroxylapophyllite-(K) is slightly less than that in fluorapophyllite-(K) (see Fig. 6) and remains less under pressure. Upon the phase transition the break on the dependence (K–O_w) – P is practically absent.

In the structure of hydroxylapophyllite-(K), similarly to the other minerals of this group, the hydrogen bonds between the H₂O molecules and the O atoms of silicate layer are differentiated. The hydrogen bond H1•••O3A with the apical O atom is strong, whereas the bond H2•••O2 with the bridge O atom of the 4-membered ring is weak (see Table S3). The changes in the hydrogen bonds system under high pressure are, however, better evaluated by the changes in the distances Ow•••O, since the X-ray methods provide low accuracy for the determination of the hydrogen positions, especially at high pressure. The pressure evolution of the Ow•••O distances is shown in Fig. 7. The pressure increase has a greater effect on the Ow•••O2 distance, which characterizes a weak hydrogen bond. In the high-pressure orthorhombic phase the system of the Ow positions splits into two sub-systems Ow1 and Ow2; the deformation of silicate layer determines small differences (0.01–0.03 Å) between the Ow•••O distances for these two sub-systems.

All structure changes are fully reversible; after the pressure release the structure returns to the initial state.

It can be stated that the compounds of the apophyllite structure type are not capable of additional hydration under pressure; this is evidenced by the behavior of both hydroxylapophyllite-(K) studied here and fluorapophyllite-(K) (Seryotkin and Ignatov 2023). Also negative are the results of the comparison of the compressibility data for hydroxylapophyllite-(K) (Fan et al. 2013) and fluorapophyllite-(K) (Seryotkin and Ignatov 2023) showing a higher resistance of the (OH)-form to the compression compared to the fluorine-bearing variety.

Figure 8 shows the evolution of the normalized unit-cell parameters of hydroxy- and fluorapophyllite-(K) as a function of P . Within 3 GPa (the region of tetragonal (OH)-form) the dependences for these two compounds coincide. Notable is only a slightly larger (by 0.1%) decrease of the c/c_0 value for hydroxylapophyllite-(K) compared to fluorapophyllite-(K); this difference persists up to 3 GPa. Above 3 GPa hydroxylapophyllite-(K) undergoes the phase transition with the symmetry lowering down to orthorhombic (space group $Pnmm$). In contrast, fluorapophyllite-(K) remains tetragonal (space group $P4/mnc$) upon the compression up to 5 GPa (Seryotkin and Ignatov 2023). Orthorhombic phase of the (OH)-form is compressed most strongly along the a axis; its compression along the b axis is comparable with the compression of the fluorine-bearing variety along the a axis (Fig. 8). At 4.6 GPa the difference between the a/a_0 and b/b_0 values for hydroxy- and fluorapophyllite comprises -0.7 and $+0.2\%$, respectively. The aforementioned growth of the compression of the orthorhombic (OH)-form along the c axis slightly increases the difference in the c/c_0 values for hydroxy- and fluorapophyllite (-0.4% at 4.6 GPa). As a result, being their compressibility comparable within 3 GPa, the pressure-induced volume contraction of the orthorhombic (OH)-form is larger compared to that of the fluorine-bearing variety: at 4.6 GPa the difference comprises -0.8% .

A rather uniform compression of these two minerals along the c axis determines also similar compression of their inter-layer spaces (Fig. 4); as regards the thickness of silicate layer, during the compression it remains practically constant in both the (OH)- and F-form. The symmetry lowering of hydroxylapophyllite-(K) structure leads to the distortion of the four-membered rings in silicate layer: in tetragonal structure these "windows" have a square shape, whereas in orthorhombic structure they are contracted along the diagonal O2–O2 more than along O20–O20 and become rhombic. Such distortion is seen in the differentiation of the angles Si–O2–Si and Si–O20–Si values (Fig. 3) and results in different compression along the axes a and b .

The systems of inter-layer cations differ only slightly in two minerals. As it was mentioned, at normal conditions the mean distance Ca– ϕ ($\phi = O, H_2O, (OH), F$) in hydroxylapophyllite-(K) is slightly larger than that in fluorapophyllite-(K) (Fig. 5). On the contrary, the K–Ow bond distances are somewhat less in the (OH)-form. Upon the compression up to 5 GPa both of these trends persist. The pressure dependences for the Ow•••O distances, characterizing hydrogen bonds, are almost identical for hydroxy- and fluorapophyllite-(K) (Fig. 7). The symmetry lowering in the (OH)-form during the phase transition does not affect the course of dependencies (within the accuracy of the definition).

Conclusion

Comparative study of the high-pressure structure evolution of the apophyllite group minerals allows to evaluate the effect of the compound chemical composition on the structure reaction to the compression. In general, the behavior of layered silicates at high pressure has been poorly studied, and of the compounds of the apophyllite topological type only fluorapophyllite-(K) has previously been structurally studied at high pressure.

The X-ray single crystal diffraction method was used to study the behavior of natural hydroxyapophyllite-(K) under compression up to 5 GPa in penetrating (water-containing) medium using DAC. The mineral composition is preserved, the pressure-induced additional hydration was not found. Within 3 GPa the compression mechanism is similar to that observed in fluorapophyllite-(K): in the (*xy*) plane the compression proceeds via the relative rotation of the 4-membered rings of silicate layer; the compression along the *z* direction proceeds through the shortening of the interlayer distance, the thickness of silicate layer remaining almost constant. This explains the similarity of the u.c. metrics changes in the (OH)- and F-form in the range of 0,0001–3 GPa. Above 3 GPa the mineral undergoes a presumably 1st order phase transition with the symmetry lowering to orthorhombic (space group *Pnnm*). The angular deformation of the 4-membered rings in the orthorhombic structure determines anisotropic compression along the axes *a* and *b*, whereas the shrinkage of silicate layer defines a greater compressibility of the high-pressure phase along the *c* axis compared to tetragonal fluorapophyllite-(K). As a result, being the compressibility of hydroxy- and fluorapophyllite-(K) similar below 3 GPa, the volume of the orthorhombic (OH)-form decreases appreciably faster with pressure compared to the fluorine-bearing variety.

Declarations

Acknowledgements

This study is supported by the Russian Science Foundation (grant # 22-27-00235). The chemical analyses were carried out at the Analytical Center for Multi-Elemental and Isotope Research (Sobolev Institute of Geology and Mineralogy, Novosibirsk, Russia). X-ray experiments were done using the equipment of Research and Education Centre “Molecular Design and Ecologically Safe Technologies” at NSU.

Data availability The data that support the findings of this study are available from the corresponding author upon reasonable request.

Competing interests

The author declares no competing interests.

Conflict of interest

The author declares that he has no known competing financial interests or personal relationships that could have appeared to influence the work reported in this paper.

References

1. Agakhanov AA, Pautov LA, Kasatkin AV, Karpenko VY, Sokolova E, Day MC, Hawthorne FC, Muftakhov VA, Pekov IV, Cámara F, Britvin SN (2019) Fluorapophyllite-(Cs), $\text{CsCa}_4\text{Si}_8\text{O}_{20}\text{F}\cdot 8\text{H}_2\text{O}$, a new apophyllite-group mineral from the Darai-Pioz massif, Tien-Shan, northern Tajikistan. *Canad Miner* 57:965–971. <https://doi.org/10.3749/canmin.1900038>
2. Arletti R, Quartieri S, Vezzalini G (2010) Elastic behavior of zeolite boggsite in silicon oil and aqueous medium: A case of high-pressure-induced over-hydration. *Amer Miner* 95:1247–1256. <https://doi.org/10.2138/am.2010.3482>
3. Belitsky IA, Fursenko BA, Gabuda SP, Kholdeev OV, Seryotkin YV (1992) Structural transformations in natrolite and edingtonite. *Phys Chem Minerals* 18:497–505. <https://doi.org/10.1007/BF00205264>
4. Boehler R (2006) New diamond cell for single-crystal x-ray diffraction. *Rev Sci Instrum* 77:115103. <https://doi.org/10.1063/1.2372734>
5. Chao GY (1971) The refinement of the crystal structure of apophyllite. II. Determination of the hydrogen positions by X-ray diffraction. *Amer Miner* 56:1234–1242.
6. Colville AA, Anderson CP, Black PM (1971) Refinement of the crystal structure of apophyllite. I. X-ray diffraction and physical properties. *Amer Miner* 56:1222–1233.
7. Comodi P, Gatta GD, Zanazzi PF (2003) Effects of pressure on the structure of bikitaite. *Eur J Mineral* 15:247–255. <https://doi.org/10.1127/0935-1221/2003/0015-0247>
8. Fan D-W, Wei Sh-Y, Xie H-S (2013) An *in situ* high-pressure X-ray diffraction experiment on hydroxyapophyllite. *Chinese Phys B* 22:010702. <http://dx.doi.org/10.1088/1674-1056/22/1/010702>
9. Gatta GD, Lee Y (2007) Anisotropic elastic behaviour and structural evolution of zeolite phillipsite at high pressure: A synchrotron powder diffraction study. *Micropor Mesopor Mater* 105:239–250. <https://doi.org/10.1016/j.micromeso.2007.01.031>
10. Gatta GD, Lotti P, Tabacchi G (2018) The effect of pressure on open-framework silicates: elastic behaviour and crystal–fluid interaction. *Phys Chem Minerals* 45:115–138. <https://doi.org/10.1007/s00269-017-0916-z>
11. Kim YH, Choi J, Heo S, Jeong N, Hwang GC (2015) High pressure behavior study of the apophyllite (KF). *J Mineral Soc Korea* 28: 325–332.
12. Lavrent'ev YuG, Karmanov NS, Usova LV (2015) Electron probe microanalysis of minerals: microanalyzer or scanning electron microscope? *Russ Geol Geophys* 56:1154–1161. <https://doi.org/10.1016/j.rgg.2015.07.006>
13. Lee Y, Vogt T, Parise JB, Artioli G (2002) Pressure-induced volume expansion of zeolites in the natrolite group. *J Am Chem Soc* 124:5466–5475. <https://doi.org/10.1021/ja0255960>
14. Marriner GL, Tarney J, Langford JI (1990) Apophyllite group: effects of chemical substitutions on dehydration behaviour, recrystallization products and cell parameters. *Miner Mag* 54:567–577. <https://doi.org/10.1180/minmag.1990.054.377.06>
15. Matsueda H, Miura Y, Rucklidge J (1981) Natroapophyllite, a new orthorhombic sodium analog of apophyllite. I. Description, occurrence and nomenclature. II. Crystal structure. *Amer Miner* 66:410–423.

16. Piermarini GJ, Block S, Barnett JD, Forman RA (1975) Calibration of the pressure dependence of the R_1 ruby fluorescence line to 195 kbar. *J Appl Phys* 46:2774–2780. <https://doi.org/10.1063/1.321957>
17. Rigaku Oxford Diffraction (2022) CrysAlisPro software system, version 1.171.42.49. Rigaku Corporation, Oxford.
18. Rouse RC, Peacor DR, Dunn P J (1978) Hydroxyapophyllite, a new mineral and a redefinition of the apophyllite group. II. Crystal structure. *Amer Miner* 63:199–202.
19. Seoung D, Lee T, Kao CC, Vogt T, Lee Y (2013) Super-hydrated zeolites: pressure-induced hydration in natrolites. *Chem Eur J* 19:10876–10883. <https://doi.org/10.1002/chem.201300591>
20. Seryotkin YV (2015) Influence of content of pressure-transmitting medium on structural evolution of heulandite: single-crystal X-ray diffraction study. *Micropor Mesopor Mater* 214:127–135. <https://doi.org/10.1016/j.micromeso.2015.05.015>
21. Seryotkin YV (2016) Evolution of the bikitaite structure at high pressure: single-crystal X-ray diffraction study. *Micropor Mesopor Mater* 226:415–423. doi:10.1016/j.micromeso.2016.02.021
22. Seryotkin YV (2019) Evolution of the brewsterite structure at high pressure: a single-crystal X-ray diffraction study. *Micropor Mesopor Mater* 276:167–172. <https://doi.org/10.1016/j.micromeso.2018.09.030>
23. Seryotkin YuV (2022) High-pressure behaviour of stellerite: single-crystal X-ray diffraction study. *Phys Chem Minerals* 49:25. <https://doi.org/10.1007/s00269-022-01205-6>
24. Seryotkin YV, Bakakin VV, Fursenko BA, Belitsky IA, Joswig W, Radaelli PG (2005) Structural evolution of natrolite during over-hydration: a high-pressure neutron diffraction study. *Eur J Mineral* 17:305–313. <https://doi.org/10.1127/0935-1221/2005/0017-0305>
25. Seryotkin YV, Likhacheva AY, Rashchenko SV (2016) Structural evolution of Li-exchanged natrolite at pressure-induced over-hydration: An X-ray diffraction study. *J Struct Chem* 57:1377–1385. <https://doi.org/10.1134/S0022476616070118>
26. Seryotkin Y, Ignatov M (2023) Structure evolution of fluorapophyllite-(K) under high pressure. *High Pres Res* (in press). <https://doi.org/10.1080/08957959.2023.2248357>
27. Sheldrick G (2015) Crystal structure refinement with SHELXL. *Acta Crystallogr C Struct Chem* C71:3–8. <https://doi.org/10.1107/S2053229614024218>
28. Sokol EV, Gaskova OL, Kozmenko OA, Kokh SN, Vapnik EA, Novikova SA, Nigmatulina EN (2014) Clastic dikes of the Hatrurim basin (western flank of the Dead Sea) as natural analogues of alkaline concretes: mineralogy, solution chemistry, and durability. *Dokl Earth Sc* 459:1436–1441. <https://doi.org/10.1134/S1028334X14100122>
29. Števkó M., Sejkora J., Plášil J., Dolníček Z., Škoda R. (2020) Fluorapophyllite-(NH₄), NH₄Ca₄(Si₈O₂₀)F·8H₂O, a new member of the apophyllite group from the Večec quarry, eastern Slovakia. *Miner. Mag.* 84:533–539. <https://doi.org/10.1180/mgm.2020.44>

Figures

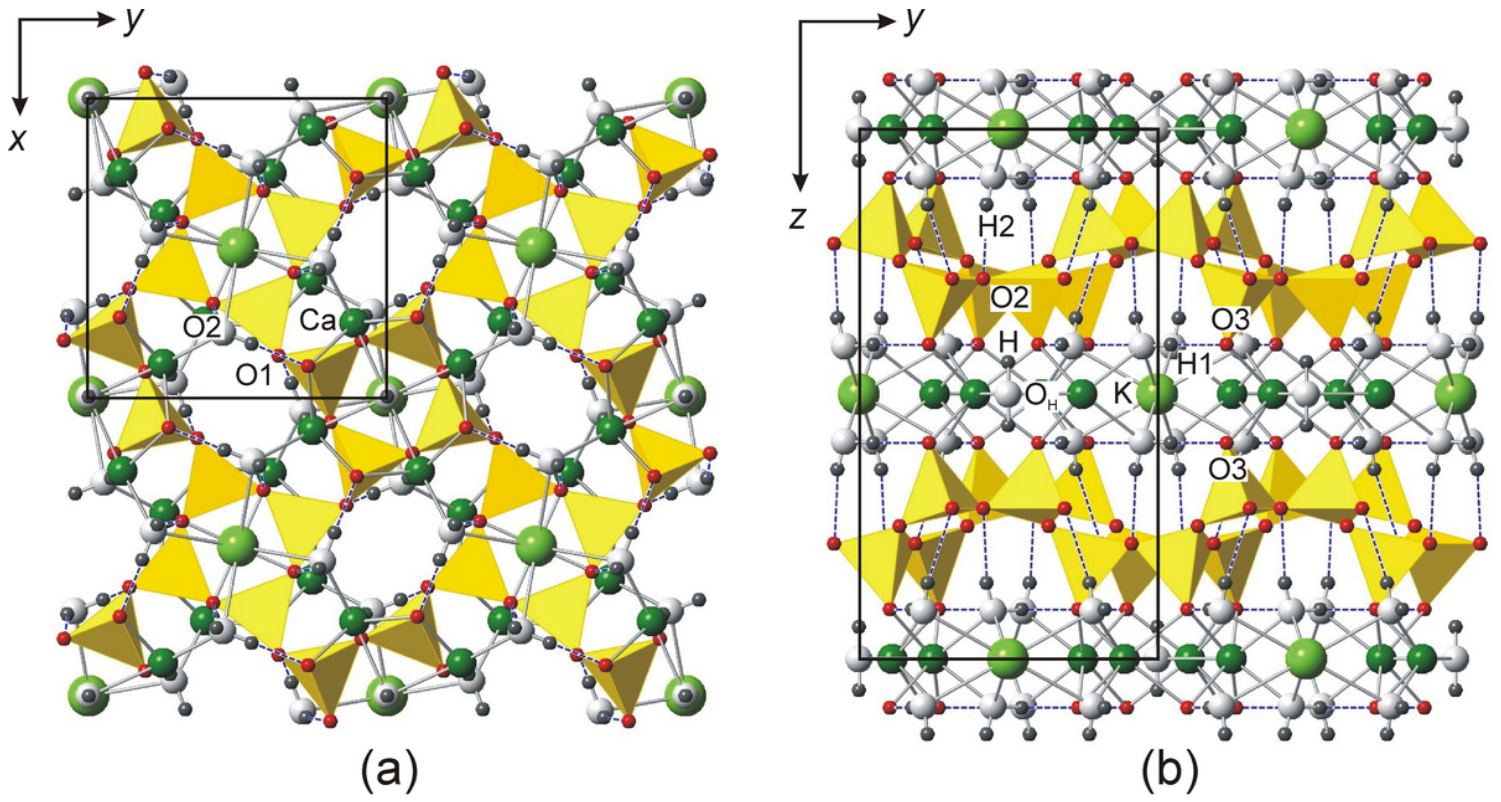


Figure 1

Crystal structure of hydroxyapophyllite-(K) projected along the c - (a) and a -axes (b).

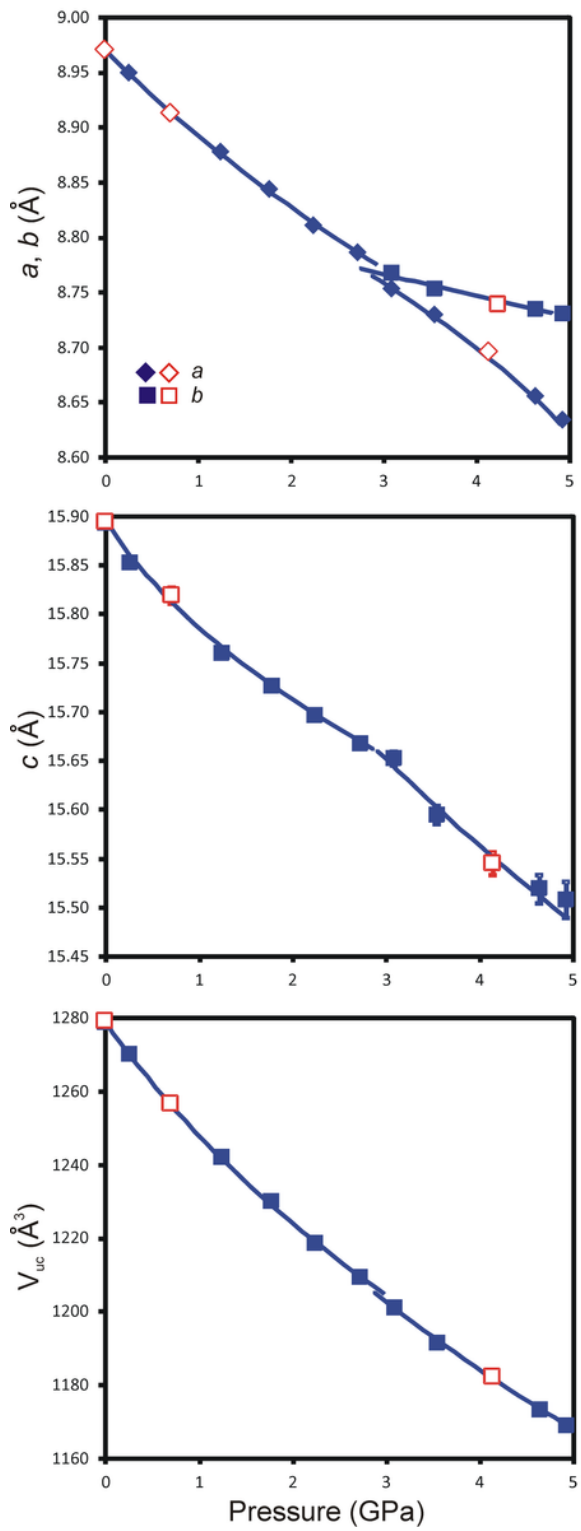


Figure 2

Lattice parameters and unit-cell volume of hydroxyapophyllite-(K) under compression (fill symbols) and under decompression (open symbols).

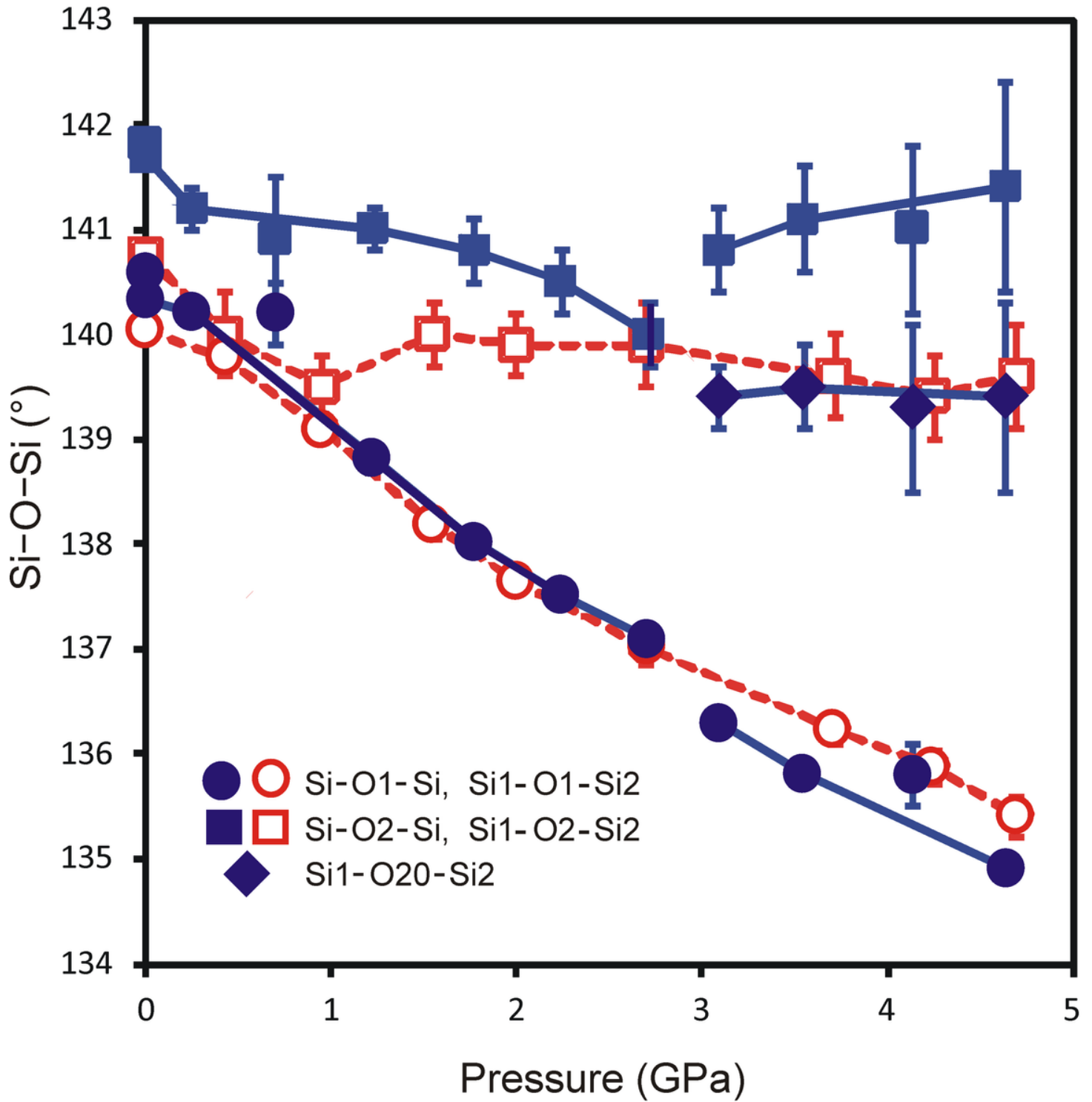


Figure 3

Si-O-Si angles changing in the structure of hydroxyapophyllite-(K) under high pressure (fill symbols) in comparison with fluorapophyllite-(K) (open symbols, Seryotkin and Ignatov 2023).

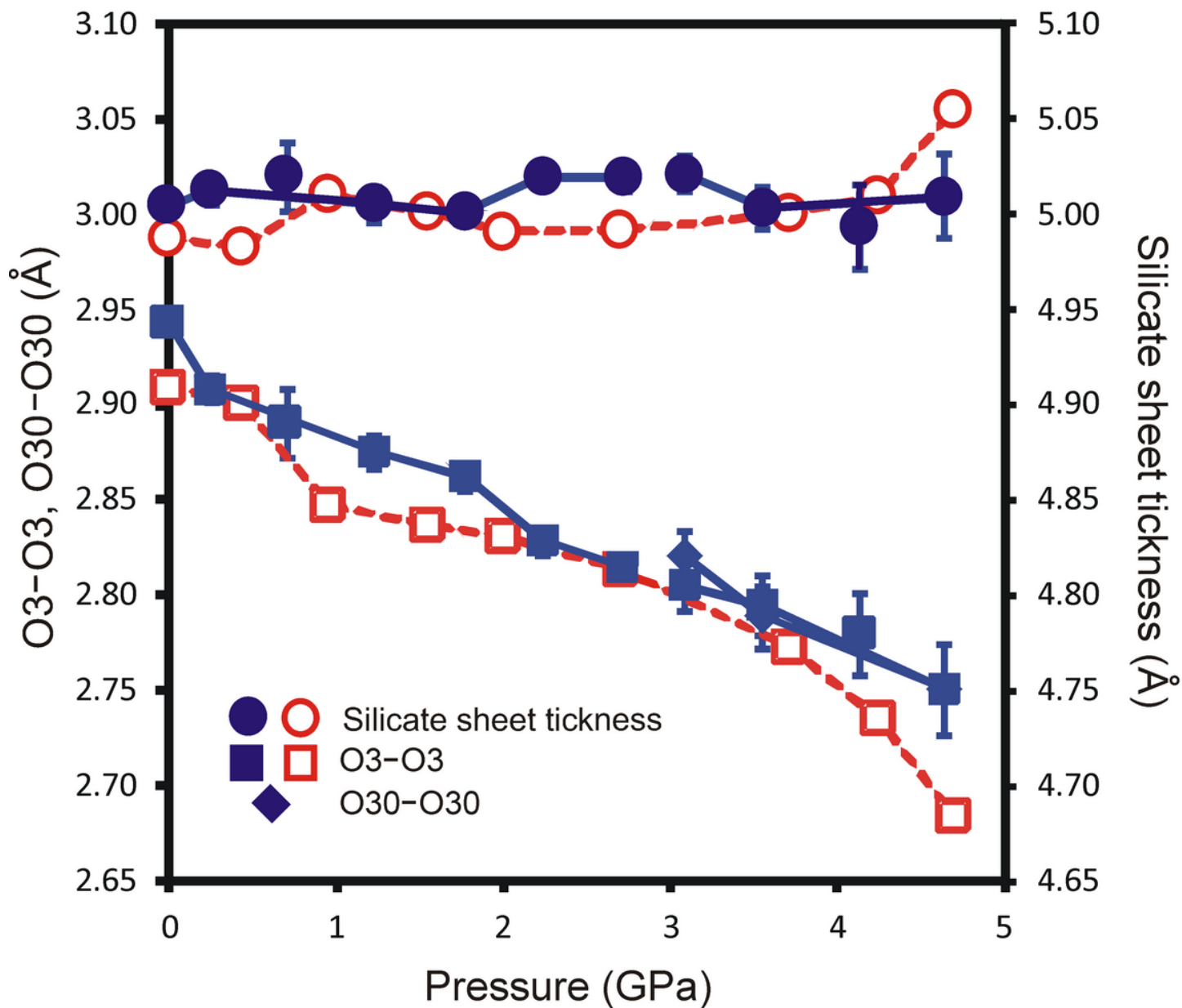


Fig. 4. The thickness of silicate sheet (●,○) and the interlayer space O3–O3 (■,□), O30–O30 (◆) under high pressure in the structure of hydrohy- (fill symbols) and fluorapophyllite-(K) (open symbols).

Figure 4

See image above for figure legend

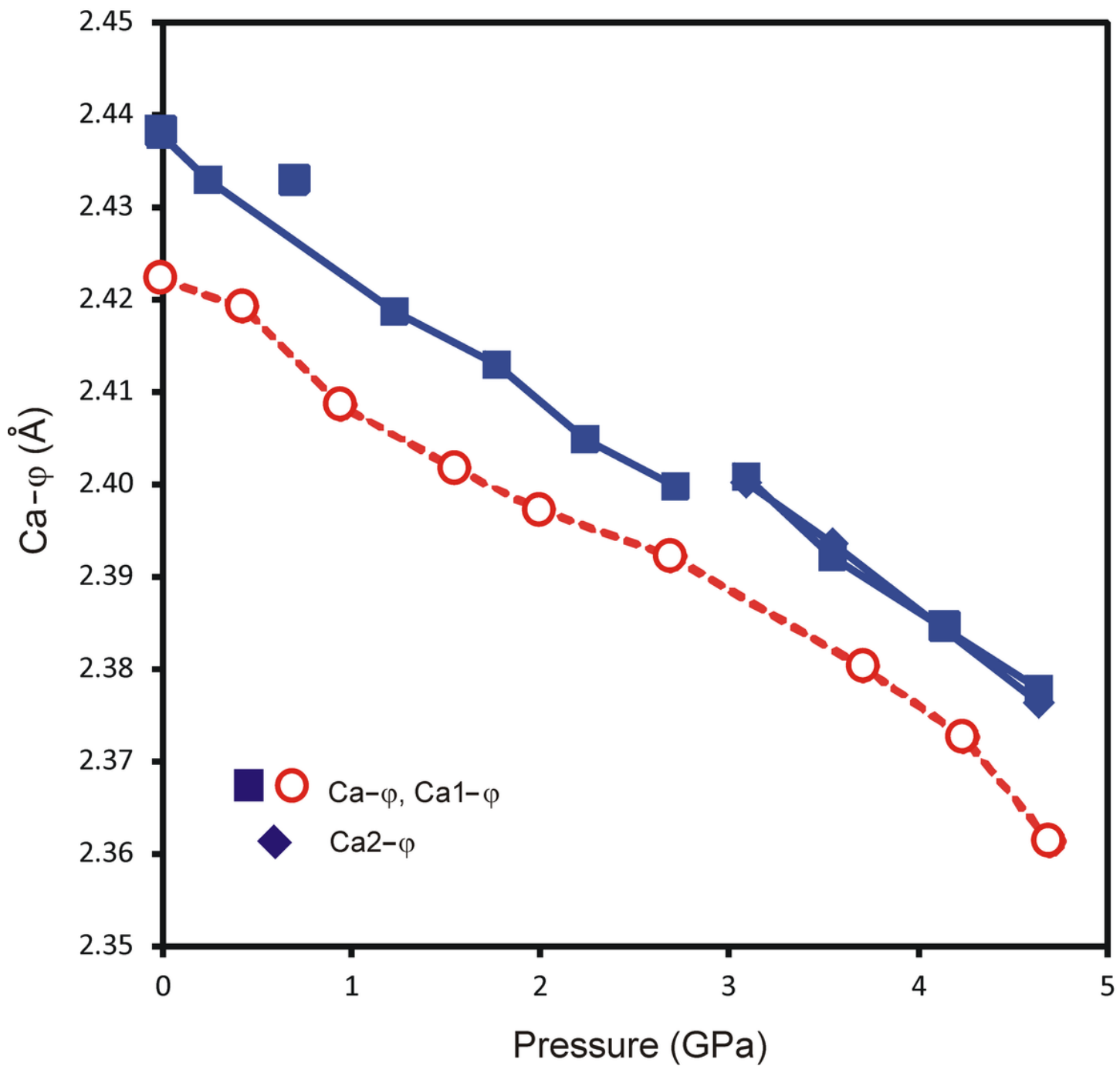


Figure 5

HP evolution of the average distance $\text{Ca}-\phi$ ($\phi = \text{O}, \text{H}_2\text{O}, (\text{OH}), \text{F}$) in coordination environment of Ca^{2+} in the structure of hydroxy- (fill symbols) and fluorapophyllite-K (open symbols).

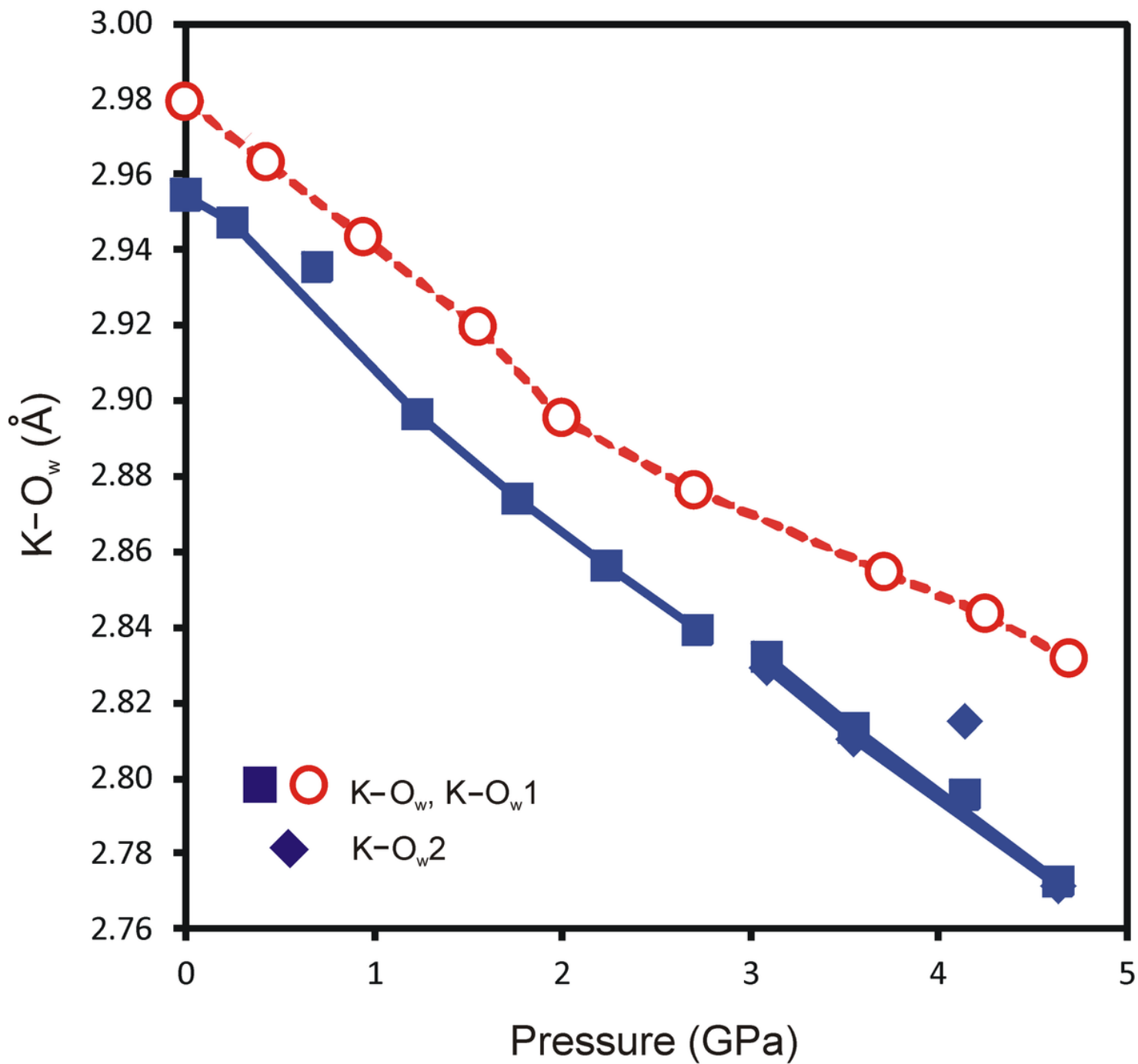


Figure 6

HP evolution of the K-O_w bond distances in the structure of hydroxy- (fill symbols) and fluorapophyllite(K) (open symbols).

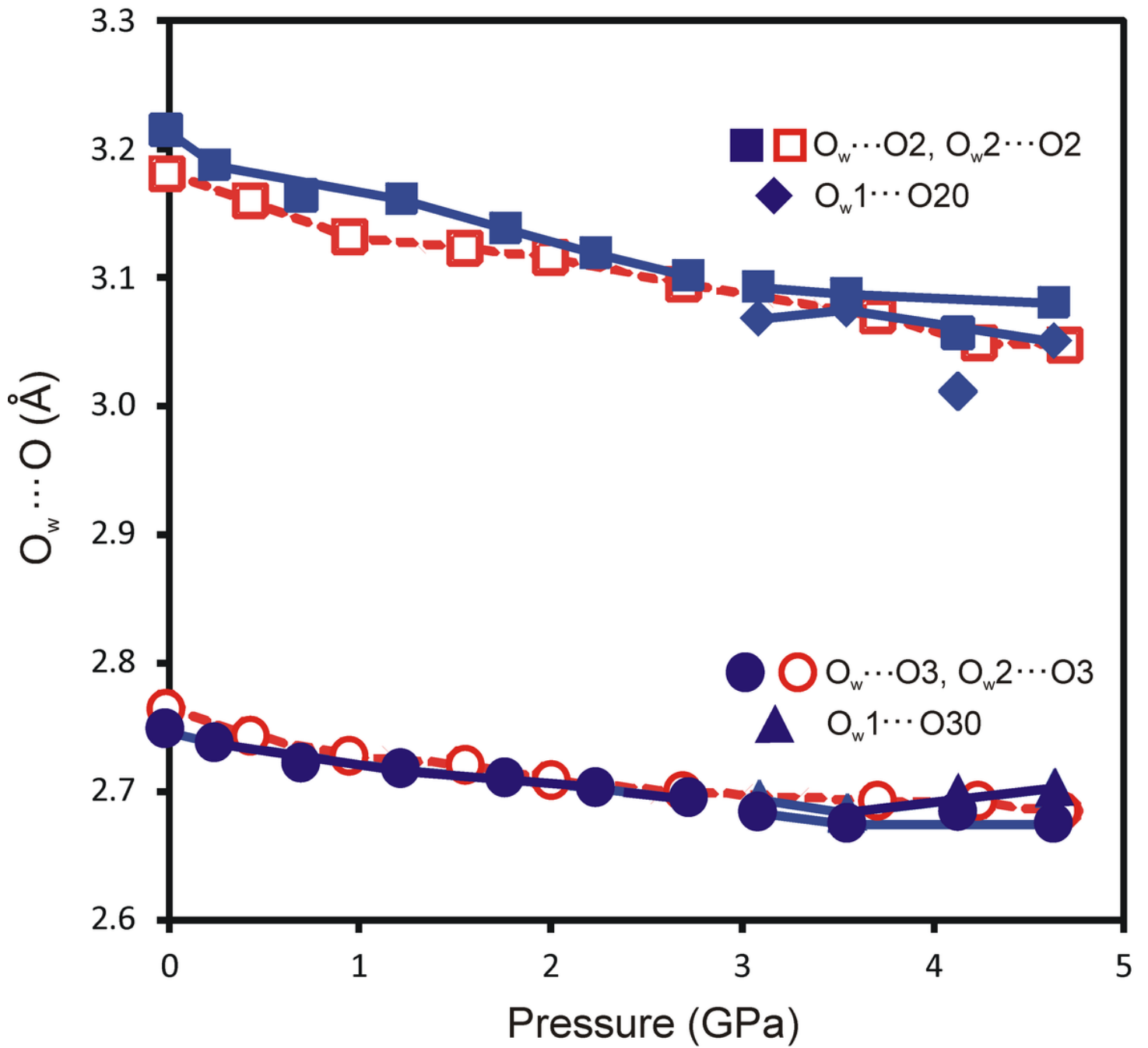


Figure 7

H_P evolution of the $O_w \cdots O$ distances in the structure of hydroxy- (fill symbols) and fluorapophyllite-(K) (open symbols).

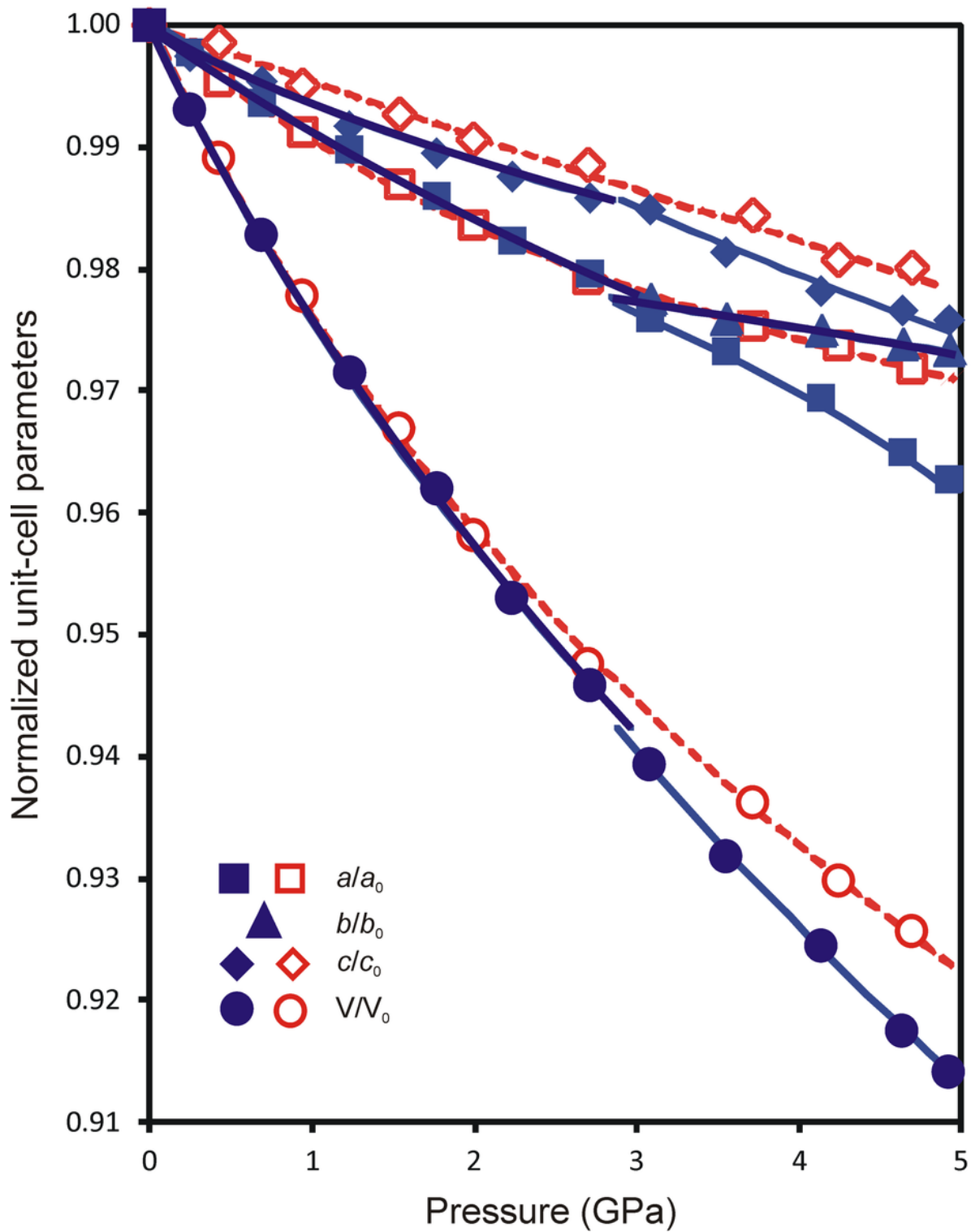


Figure 8

Normalized lattice a/a_0 , b/b_0 , and c/c_0 parameters and the unit-cell volume V/V_0 of hydroxy- (fill symbols) and fluorapophyllite-(K) (open symbols).

Supplementary Files

This is a list of supplementary files associated with this preprint. Click to download.

- [SupplTables.docx](#)
- [cifs.zip](#)